

Predicting beam and diffuse horizontal irradiance using Fourier expansions



A. Barbón^a, P. Fortuny Ayuso^b, L. Bayón^{b,*}, J.A. Fernández-Rubiera^a

^a Department of Electrical Engineering, University of Oviedo, Spain

^b Department of Mathematics, University of Oviedo, Spain

ARTICLE INFO

Article history:

Received 9 January 2020

Received in revised form

27 February 2020

Accepted 28 February 2020

Available online 6 March 2020

Keywords:

Clear sky model

Beam and diffuse horizontal irradiance

Fourier series correction

ABSTRACT

A new method for obtaining very accurate models to predict the Beam and Diffuse Horizontal Irradiance is proposed, using two sources of data: satellite irradiation estimations and two clear-sky models (one for Beam and one for Diffuse Irradiance). By means of a Fourier Series approximation, we correct the clear-sky models and adapt them to the climatological conditions of a specific location. Applying it to six cities in latitudes ranging from 36° to 60° degrees North, we compare our predictions with real ground-level data obtained (in this work) from the WRDC database. Results show that the proposed model is both accurate and applicable to different climates.

© 2020 Elsevier Ltd. All rights reserved.

1. Introduction

The power generated by renewal energy sources has increased by 14% in 2018 with respect to 2017; solar energy, in particular, has been increasing steadily in the last years and is now up to 24% higher than in 2013 [1]. The European Union has proposed to achieve a 27% share of renewable energy by 2030 [2].

Solar generated energy (both photovoltaic and thermal) depends on a large number of factors, which can be grouped into three main areas: the Earth's geometry (rotation, revolution around the Sun, latitude, longitude ...), terrain (shadows, elevation, surface inclination ...) and atmospheric attenuation (scattering, absorption by air molecules, clouds, ozone, aerosols, CO₂...) [3,4]. This makes it practically impossible to have a single global model for solar irradiance [5]. Among the existing ones, there are empirical models [6], satellite-derived ones [7], those using numerical weather predictions [8], and nowadays, some derived from artificial intelligence techniques [9]. They differ in their simplicity, accuracy, and their use or not of available meteorological data [10].

Numerous models for predicting beam and diffuse horizontal irradiance are based on the assumption of a clear day [11–18]. This assumption represents the nominal operating conditions of Concentrated Solar Power (CSP) systems [19]. By elementary

geometrical considerations, they derive a formula for the daily irradiance (beam and diffuse). However, as they do not even take into account the appearance of clouds, their estimations cannot be taken as a *true* expectation.

Maafi et al. [20] deal with cloudiness by classifying the days in three groups: clear sky, partly-cloudy and overcast. Bone et al. [21] present an intra-hour beam horizontal irradiance prediction system at the specific location of the University of Queensland. They use the clear-sky Ineichen model [22] and a cloud fraction prediction algorithm, taking advantage of an enhanced “sector-ladder” method [23]. Kostic et al. [24] present an empirical model for estimating solar insolation at a location in Serbia, using the ASHRAE clear-sky model [12], meteorological data on cloudiness, and measurements of global solar irradiance on a horizontal surface. Petrzala et al. [25] propose a clear-sky physical model for the calculation of solar irradiances at the NREL Solar Radiation Research Laboratory located in Golden, Colorado. Their system uses a model for computing the solar resources under clear-sky conditions with arbitrary turbidity. Nou et al. [19] provide a clear sky model for the calculation of beam normal irradiance, using the model developed by the PROMES-CNRS laboratory for a real-time sky imaging application. In Ref. [26], the authors develop a simulation of historical global horizontal irradiance and beam normal irradiance of solar resources in California. This system uses the REST2 clear-sky model and the MODIS level 3 (L3) daily satellite data as input. Dazhi et al. [27] use the Adnot clear-sky model presented by Ianetz et al. [28] for estimating clear sky global horizontal

* Corresponding author.

E-mail address: bayon@uniovi.es (L. Bayón).

Nomenclature			
A	Height above sea level of the location (Km)	I_{bh}	Adjusted beam solar irradiance on a horizontal plane (W/m^2)
a_0, a_i, b_i	Fourier coefficients (dimensionless)	I_{dh}	Adjusted diffuse solar irradiance on a horizontal plane (W/m^2)
E_0	Excentricity correction factor of the Earth's orbit (dimensionless)	I_0	Extraterrestrial solar irradiance (W/m^2)
\bar{H}_{ba}^m	Actual monthly averaged daily beam solar irradiation on a horizontal plane (Wh/m^2ay)	I_{SC}	Solar constant (W/m^2)
\bar{H}_{da}^m	Actual monthly averaged daily diffuse solar irradiation on a horizontal plane (Wh/m^2ay)	k_0, k_1, k	Hottel empirical constants (dimensionless)
H_{ba}	Actual daily beam solar irradiation on a horizontal plane (Wh/m^2)	l	Interval of length of interval Fourier series (rad)
H_{da}	Actual daily diffuse solar irradiation on a horizontal plane (Wh/m^2)	n	Ordinal of the day (day)
H_{bf}	Fourier model of beam solar irradiation on a horizontal plane (Wh/m^2)	PC_b^n	Daily perturbation coefficient for beam irradiance (dimensionless)
H_{df}	Fourier model of diffuse solar irradiation on a horizontal plane (Wh/m^2)	PC_d^n	Daily perturbation coefficient for diffuse irradiance (dimensionless)
H_{bh}	Beam solar irradiation on a horizontal plane transmitted through clear atmospheres (Wh/ m^2)	S	Fourier series
H_{dh}	Diffuse solar irradiation on a horizontal plane transmitted through clear atmospheres (Wh/ m^2)	T	Solar time (h)
\bar{H}_{bs}^m	Satellite estimated monthly averaged daily beam solar irradiation on a horizontal plane (Wh/ m^2ay)	T_R	Sunrise solar time (h)
\bar{H}_{ds}^m	Satellite estimated monthly averaged daily diffuse solar irradiation on a horizontal plane (Wh/ m^2ay)	T_T	Sunset solar time (h)
I_{bh}	Theoretical beam solar irradiance on a horizontal plane (W/m^2)	α_S	Height angle of the Sun (rad)
		γ_S	Azimuth of the sun (rad)
		δ	Solar declination (rad)
		θ_z	Zenith angle of the Sun (rad)
		λ	Latitude angle (rad)
		Γ	Day angle (rad)
		τ_b	Atmosphere transmittance beam irradiance (dimensionless)
		τ_d	Atmosphere transmittance diffuse irradiance (dimensionless)
		ω	Hour angle (rad)
		ω_S	Sunset hour angle (rad)
		ω_S^T	Sunset hour angle (h)

irradiance at a location in Singapore. Most of these models use data at the specific location they study and do not claim —by themselves— any generality.

Furthermore, many of the already existing models in the literature aim just for short-term forecasting of solar irradiance. For instance Ref. [29], predicts solar irradiance only several minutes in advance, using regression techniques to provide a likely clearness index. Similarly [30,31], use neural networks also for short-term predictions (between 1 and 6 h). In Refs. [32], a time-series model is used to forecast solar irradiance after sunrise. Our method provides a continuous model valid all through the year.

Other studies are based on data compiled by ground-level meteorological stations. For example [33], tries to predict solar irradiance on inclined surfaces using sky radiance data in Hong Kong. Again [31], uses observations from neighboring stations within a 55 km radius [34]; uses several datasets (air temperature, relative humidity, irradiance, etc.) at Jeddah (Saudi Arabia), for local forecasting. However, ground-based measurements are usually unavailable. Our method solves this issue by using satellite estimations, as explained in what follows.

We present in this paper a novel technique for estimating beam and diffuse solar irradiance on a horizontal surface at ground level, at any location, with any temporal resolution. Notice that the accuracy of our method diminishes when increasing the temporal resolution. However, it does provide an explicit continuous function, something which may be useful in computations.

First of all, we remark that our starting data is the monthly average of daily beam solar irradiation on an horizontal surface, computed as the difference between global and diffuse solar irradiations. As most locations lack a physical weather station, we

obtain these initial data from one of the satellite radiation tools available on the Internet. This is one of the main advantages of our approach: we only need 12 starting values (one per month), computed from estimation models. In this specific work, we use the Photovoltaic Geographical Information System (PVGIS) [35], a well known and respected system which provides information on solar radiation and photovoltaic (PV) system performance. Developed by the European Commission Joint Research Centre, it is accessible as a web application. Other options for obtaining this data are: The US National Renewable Energy Agency (NREL), which maintains the National Solar Radiation Database (NSRDB) [36]; SOLCAST [37], a global solar database produced using a range of geostationary meteorological satellites; and Meteororm [38], although this one uses a different method to model the solar resources, based on interpolated and synthetic data, instead of the satellite-derived one we use.

Secondly, notice that our aim is to adapt the clear-sky models in order to obtain better predictions for beam and diffuse solar irradiance. To this end, we compute the Fourier series of the monthly average beam solar irradiation as a predictor, and compare this value with the one provided by the theoretical clear-skies model (in our case, the Hottel model [14] and the Liu-Jordan model [15] for beam and diffuse radiation, respectively). Calculating the ratio between both values for each day, we obtain a perturbation coefficient which is applied to the solar irradiance model, providing our perturbed model.

Fourier series [39] are widely used for modeling periodic data and are very well suited for problems showing seasonality and smooth trends (as the weather tends to behave throughout the year), due to the periodic nature of the sine and cosine functions

[40]. They have already been used in the area of solar irradiation by Spencer to calculate the solar declination [41], and the eccentricity correction factor of the Earth's orbit. To our knowledge, the only previous application of Fourier series to modeling solar irradiance is [42], which uses two temporal harmonics and tries to obtain a universal model for all latitudes but only for the *global* radiation.

Our model does not intend to accurately predict cloudiness: what it does is to (roughly speaking) “distribute” the cloudiness throughout the year according to the real data (monthly means), using the Fourier Transform, which presents (as can be seen in the figures of Sections 3 and 4) a rather good fit and especially a remarkable similarity in the seasonality of the yearly distribution. Succinctly, our method takes the 12 estimated values of monthly average solar irradiation (obtained from the GIS database) and, using a Fourier Series development, computes a “tentative fitting curve”. This fitting curve is compared to the theoretical model and a daily perturbation coefficient is obtained, which permits an accurate estimation of *true* irradiance in any time frame. In this paper we apply the technique to six places *at which weather stations are deployed* belonging to different latitudes and we compare the values we obtain with the true experimental data given by those weather stations at ground level.

There are several databases providing ground-level data. Among them:

1. The Baseline Surface Radiation Network (BSRN) [43], which provides observations for short- and long-wave surface radiation fluxes, obtained from a small number of selected stations, currently 64, in contrasting climatic zones.
2. The Global Energy Balance Archive (GEBA) [44]. This is a centralized database for worldwide instrumentally measured energy fluxes at surface level. GEBA stores monthly means of the various energy flux components observed at a collection of stations.
3. The World Radiation Data Centre (WRDC) [45], which collects and archives radiometric data from all over the world. Most of the data are monthly averages, but there are daily values for some stations.

We have used the last one in our work, due to its accessibility and ease of use. Obviously, any other database can be used interchangeably.

Despite the technical nature of our approach, it has several remarkable features:

1. It is universal in the model: it can be applied readily to any clear-sky model without any essential modification (the fact that we use it for the Hottel or Liu-Jordan models is due just to simplicity in the exposition).

$$\delta = 0.006918 - 0.399912 \cdot \cos \Gamma + 0.070257 \cdot \sin \Gamma - 0.006758 \cdot \cos 2\Gamma + 0.000907 \cdot \sin 2\Gamma - 0.002697 \cdot \cos 3\Gamma + 0.001480 \cdot \sin 3\Gamma \quad (1)$$

2. It is universal in the geographical location: even if there is no true ground-level data, it can be applied to any location and climatological conditions, using just satellite estimations.
3. It is readily implementable: we give a precise description and the data we use is freely available (from the database we use or from others). Moreover, only 12 input pairs are necessary.

4. The computations are easy to program and the final expression of the model is just the original one multiplied, each day, by a coefficient.
5. Finally, the perturbed model one obtains is continuous on the day of the year, a property of the theoretical model which is important to preserve.

As we show in Section 3, our method predicts the true values with great accuracy. The results are not only valid at the monthly scale (i.e. monthly averages) but also at the daily scale. This is due to the very good fit provided by Fourier Series in general and to the fact that we obtain a continuous function, which admits discretization to any scale.

The paper is organized as follows. First, we present the proposed method theoretically. Then we develop it in detail for the specific case of a location: Wien (Austria). Afterwards, we show the (summarized) results obtained at other locations: Desert Rock (USA), Rock Springs/Penn State (USA), Valentia (Ireland), Tartu (Estonia) and Lerwick (UK), so that a wide range of latitudes in the Northern Hemisphere is covered. Finally, we provide a detailed statistical study of the errors of our perturbed model with respect to actual experimental data, both at the monthly and daily scales. Conclusions and future perspectives end this work.

2. Description of the method

Our proposed method is based on the following steps:

1. Fix a clear-sky irradiance model. In this paper, by way of illustration, we have used the Hottel model for beam and the Liu-Jordan for diffuse irradiance, respectively, its extension to others being evident.
2. Using the satellite (estimated) solar irradiation data available for the city under study, compute the Fourier series of the monthly average beam solar irradiation on a horizontal surface.
3. Compute the daily quotient between the Fourier series and the values of daily irradiation given by the clear-sky model to obtain a perturbation coefficient.
4. Multiply the clear-sky irradiance model by the perturbation coefficient to obtain the perturbed model (i.e. the “cloudy-skies irradiance model”).

2.1. Two classic clear-sky models

Let us review the main parameters we shall use in this work. The two main constants for each location are its latitude λ and elevation A . The solar declination δ (rad) for the n -th day of the year is given, approximately, by (see Ref. [41]):

where Γ (rad) is the day angle, defined as:

$$\Gamma = (n - 1) \frac{2\pi}{365} \quad (2)$$

The eccentricity correction factor of the Earth's orbit E_0

(dimensionless), can also be found in Ref. [41]:

$$E_0 = 1.000110 + 0.034221 \cdot \cos \Gamma + 0.001280 \cdot \sin \Gamma + 0.000719 \cdot \cos 2\Gamma + 0.000077 \cdot \sin 2\Gamma \quad (3)$$

This value is used to compute the irradiance incident on a plane normal to the radiation (again, [41]):

$$I_0 = I_{SC} \cdot E_0 \quad (4)$$

where I_0 (W/m^2) is the extraterrestrial solar irradiance on the plane normal to the radiation, on the n -th day of the year, and $I_{SC} = 1367$ (W/m^2) is the solar constant.

The sunset hour angle ω_S (for each day n) is equal to (see Ref. [46]):

$$\omega_S = \arccos(-\tan(\delta) \cdot \tan(\lambda)) \quad (5)$$

where δ (rad) is the solar declination, and λ (rad) is the latitude (rad). The sunrise hour angle is the negative of the sunset hour angle. In hours (h), we have:

$$\omega_S^T = \omega_S(180 / (\pi \cdot 15)) \quad (6)$$

From which the sunrise T_R and sunset T_S (both in h) solar times are calculated (see Ref. [47]):

$$T_R = 12 - \omega_S^T \quad (7)$$

$$T_S = 12 + \omega_S^T \quad (8)$$

The hour angle ω (rad) is defined as (see Ref. [47]):

$$\omega = ((\pi \cdot 15) / 180) \cdot (T - 12) \quad (9)$$

where T (h) is the solar time.

The height angle of the sun α_S (rad) can be found in Ref. [47]:

$$\alpha_S = \arcsin[\sin \delta \sin \lambda + \cos \delta \cos \lambda \cos \omega] \quad (10)$$

Finally, the zenith angle of the sun, θ_z (rad) is the complementary of α_S :

$$\theta_z = \pi/2 - \alpha_S \quad (11)$$

2.1.1. Beam clear-sky irradiance

We choose the classic and well-known Hottel [14] model for beam clear-sky irradiance as the starting point. The process to follow is totally similar for any other model.

The atmospheric transmittance τ_b is defined as the ratio between the beam solar irradiance received on the surface of the Earth and the extraterrestrial solar irradiance incident on a plane normal to the radiation. It is modeled using the zenith angle and altitude for a standard atmosphere and four types of climate. Its formula is:

$$\tau_b = k_0 + k_1 \cdot e^{-k/\cos \theta_z} \quad (12)$$

where, θ_z (rad) is the zenith angle of the sun, τ_b (dimensionless) is the atmosphere transmittance for beam solar irradiance for any θ_z , and the parameters k_0 , k_1 , and k are empirical constants for a standard atmosphere with 23 (km) of visibility, which are:

$$k_0 = 0.4237 - 0.00821(6 - A)^2 \quad (13)$$

$$k_1 = 0.5051 - 0.0059(6.5 - A)^2 \quad (14)$$

$$k = 0.2711 - 0.01858(2.5 - A)^2 \quad (15)$$

where, A (km) is the elevation above sea level of the location. Notice that when $A \leq 2.5$ (km), the above values for k_0 , k_1 , and k are multiplied respectively by three correction factors r_0 , r_1 and r_k , tabulated in Ref. [14] for four types of climate. The Hottel model has been used extensively [48–50].

The beam solar irradiance on a horizontal plane transmitted through clear atmospheres is given by:

$$I_{bh} = I_0 \cdot \cos \theta_z \cdot \tau_b \quad (16)$$

Equation (16) allows the calculation of the hourly distribution $I_h(n, T)$ (W/m^2) of beam solar irradiance on a horizontal plane transmitted through clear atmospheres. This distribution is a curve that provides the I_h for the Hottel model, for each day n of the year, as a function of the solar time of day, T :

$$I_{bh}(n, T) = I_0(n) \cdot \cos \theta_z(n, T) \cdot \tau_b(n, T) \quad (17)$$

Note that the we implement the Hottel model using the standard values of the coefficients proposed in Ref. [14].

The daily distribution $H_{bh}(n)$ ($\text{W} \cdot \text{h}/\text{m}^2$) of beam solar irradiation on a horizontal plane transmitted through clear atmospheres is obtained by integrating through a whole day, from sunrise to sunset, the hourly irradiance distribution $I_h(n, T)$ (i.e. calculating the area under the irradiance curve):

$$H_{bh}(n) = \int_{T_R(n)}^{T_S(n)} I_{bh}(n, T) dT \quad (18)$$

2.1.2. Diffuse Irradiance

Liu and Jordan [15] provide an empirical relation between the transmission coefficients of beam and diffusive solar irradiance for clear skies:

$$\tau_d = 0.271 - 0.294 \cdot \tau_b \quad (19)$$

where τ_b is the atmosphere transmittance for beam solar irradiance (dimensionless) for any θ_z , determined using the Hottel model and τ_d is the atmosphere transmittance for diffuse solar irradiance (dimensionless) for any θ_z . Their model has been used, among others, by Ref. [48,49], and [50].

The diffuse solar irradiance on a horizontal plane, is given by the model as:

$$I_{dh}(n, T) = I_0(n) \cdot \cos \theta_z(n, T) \cdot \tau_d(n, T) \quad (20)$$

where I_0 is the extraterrestrial solar irradiance, measured on the plane normal to the radiation (W/m^2), θ_z is the zenith angle of the sun, and τ_d is the atmosphere transmittance for diffuse solar irradiance (dimensionless) for any θ_z .

The daily distribution $H_{dh}(n)$ ($\text{W} \cdot \text{h}/\text{m}^2$) of diffuse solar irradiation on a horizontal plane transmitted through clear atmospheres is obtained performing the corresponding integral:

$$H_{dh}(n) = \int_{T_R(n)}^{T_S(n)} I_{dh}(n, T) dT \quad (21)$$

2.2. Satellite data of solar irradiation

We are going to use the satellite estimation of monthly average daily solar irradiation (both beam and diffuse) on a horizontal plane, datum which we obtain using the PVGIS database (period of 10 years (2005 – 2014)) [35]. The value for the monthly average of daily diffuse irradiation $\overline{H}_{ds}^m(n)$ ($W \cdot h/m^2$ /day), for each month m of the year, is provided directly by the database. However, the monthly average of daily beam solar irradiation $\overline{H}_{bs}^m(n)$ ($W \cdot h/m^2$ /day), for each month m of the year, must be calculated from the PVGIS data by subtracting from the global solar irradiation the diffuse term.

2.3. Fourier Series approximation

Notice that the functions $\overline{H}_{bs}^m(n)$ and $\overline{H}_{ds}^m(n)$ are step functions (they are constant on each month). For the sake of clarity, in this section, we shall refer to both as $\overline{H}_s^m(n)$ (as the algorithm is the same, only the initial data are different).

We are going to compute the Fourier expansion (obviously, truncated) of $\overline{H}_s^m(n)$ to get a continuous adjusted model of daily irradiation.

Recall that a Fourier series [39] in the variable n is an expression:

$$S(n) = \frac{a_0}{2} + \sum_{i=1}^{\infty} \left(a_i \cos \frac{\pi i n}{l} + b_i \sin \frac{\pi i n}{l} \right) \quad (22)$$

and that, given any piecewise-continuous periodic function $f(n)$ with period $2l$, there is a Fourier series $S(n)$ converging to $f(n)$ for all n (except possibly at the points of discontinuity). In fact, the coefficients a_i and b_i for $f(n)$ take the following values:

$$a_0 = \frac{1}{l} \int_{-l}^l f(n) dn$$

$$a_i = \frac{1}{l} \int_{-l}^l f(n) \cos i \frac{\pi}{l} n \, dn; \quad i = 1, 2, \dots \quad (23)$$

$$b_i = \frac{1}{l} \int_{-l}^l f(n) \sin i \frac{\pi}{l} n \, dn; \quad i = 1, 2, \dots$$

However, our functions $\overline{H}_s^m(n)$ are not periodic (they are defined only for $n \in [0, 365]$). The usual technique to deal with functions defined on a compact interval is to “make them periodic” by repeating them on each interval of length l . In our case, for the sake of simplicity and to avoid convergence issues, we choose to extend it in an even way, by defining $\widehat{H}_s^m(n) = \overline{H}_s^m(n)$ for $n \in [0, 365]$, and then:

$$\widehat{H}_s^m(-n) = \overline{H}_s^m(n) \quad (24)$$

for $n \in [-365, 0]$ and finally, copying this behavior for $n \in [-365, 365]$ periodically in \mathbb{R} . This way, we obtain a (notice here

that there is one for the beam irradiation and one for the diffuse) piecewise-continuous periodic function defined on all of \mathbb{R} , whose Fourier series we can compute using (23). It is well-known [40] that the Fourier coefficients b_i (23) of an even function are 0: the corresponding series is called a cosine series. As we only have essentially 12 data points (one for each month), the Nyquist-Shannon sampling theorem [40] implies that only the first 12 coefficients are relevant; we are going to restrict ourselves to those 12 initial terms of the series, thus obtaining a trigonometric polynomial in $\cos(i\pi n/l)$ for $i = 1, \dots, 12$. Therefore, we compute:

$$a_0 = \frac{2}{365} \int_0^{365} \overline{H}_s^m(n) \, dn$$

$$a_i = \frac{2}{365} \int_0^{365} \overline{H}_s^m(n) \cos \frac{\pi i n}{365} \, dn, \quad i = 1, 2, \dots, 12 \quad (25)$$

$$b_i = 0$$

From the above computations, we obtain the Fourier model $H_f(n)$ (truncation of the corresponding Fourier series $S(n)$):

$$H_f(n) = a_0 + a_1 \cos \frac{\pi n}{365} + a_2 \cos \frac{2\pi n}{365} + \dots + a_{12} \cos \frac{12\pi n}{365} \quad (26)$$

defined for $n \in [0, 365]$ (actually defined on all of \mathbb{R} but we are only interested on the values for each day of the year).

At this point (after performing the computations for beam and diffuse irradiations), we have two approximating functions, which we call $H_{bf}(n)$ (for the beam solar irradiation) and $H_{df}(n)$ (for the diffuse solar irradiation).

These functions $H_{bf}(n)$ and $H_{df}(n)$ are now respectively compared to the clear-sky daily irradiation distributions $H_{bh}(n)$ and $H_{dh}(n)$ given by the Hottel and the Liu-Jordan models in order to obtain the daily perturbation coefficients (dimensionless):

$$PC_b^n = \frac{H_{bf}(n)}{H_{bh}(n)}; \quad PC_d^n = \frac{H_{df}(n)}{H_{dh}(n)} \quad (27)$$

(one for each day of the year). These are the coefficients we use to finally compute the adjusted hourly distribution of beam and diffuse horizontal solar irradiance [47]:

$$\mathbb{I}_{bh}(n, T) = I_{bh}(n, T) \cdot PC_b^n \quad (28)$$

$$\mathbb{I}_{dh}(n, T) = I_{dh}(n, T) \cdot PC_d^n \quad (29)$$

3. Examples

In order to provide a full explanation of our method, we are going to apply it in complete detail to Wien, one of the six cities we

Table 1
Cities under study.

	City	Latitude	Longitude	Elevation
1	Desert Rock (USA)	36°37'00" N	116°01'00" W	1007 (m)
2	Rock Springs/Penn State (USA)	40°43'00" N	77°56'00" W	376 (m)
3	Wien (Austria)	48°15'00" N	16°21'00" E	203 (m)
4	Valentia (Ireland)	51°48'00" N	10°15'00" W	14 (m)
5	Tartu (Estonia)	58°15'00" N	26°28'00" W	70 (m)
6	Lerwick (UK)	60°08'00" N	1°11'00" W	63 (m)

have chosen. The other five will be summarily covered. We have chosen six cities for the sake of brevity with the aim of covering a large range of latitudes in the Northern Hemisphere. Table 1 shows the geographic characteristics of the cities under study.

3.1. Detailed example: Wien

The latitude of Wien is $48^{\circ}15'00''$ N, so that $\lambda = 0.842$ (rad), and its height above sea level is $A = 0.203$ (km). Moreover, the hourly distribution $I_{bh}(n, T)$ (W/m^2) of beam solar irradiance for the Hottel model in this type of climate requires the following three correction coefficients: $r_0 = 0.97$, $r_1 = 0.99$ and $r_k = 1.02$, per [14].

The first step in the proposed method is to gather the monthly averages of irradiation from the PVGIS database. For the 10 years 2005–2014, we get the lists:

$$\bar{H}_{bs}^m = [386.86, 679.12, 1778.81, 2634.88, 3086.32, 3033.07, 3485.82, 2841.15, 1977.04, 1192.83, 391.91, 320.29] \quad (30)$$

$$\bar{H}_{ds}^m = [615.95, 872.92, 1645.52, 1981.22, 2424.92, 2555.19, 2515.35, 2081.21, 1590.25, 1130.67, 658.61, 535.24] \quad (31)$$

Following the method of Section 2, we compute the corresponding Fourier expansions. Writing, as is usual,

$$\hat{\omega} = \frac{\pi}{l} = \frac{\pi}{365} \quad (32)$$

which is twice the frequency of the fundamental harmonic, we obtain (rounding to two decimal digits):

$$\begin{aligned} H_{bs}^m \sim H_{bf}(n) = & 1764.84 + 204.24\cos(\hat{\omega}t) - 1510.84\cos(2\hat{\omega}t) - 121.16\cos(3\hat{\omega}t) \\ & - 55.62\cos(4\hat{\omega}t) - 125.40\cos(5\hat{\omega}t) + 62.67\cos(6\hat{\omega}t) + 83.40\cos(7\hat{\omega}t) + 54.29\cos(8\hat{\omega}t) \\ & - 58.61\cos(9\hat{\omega}t) + 43.61\cos(10\hat{\omega}t) + 50.19\cos(11\hat{\omega}t) + 16.55\cos(12\hat{\omega}t) \end{aligned} \quad (33)$$

$$\begin{aligned} \bar{H}_{ds}^m \sim H_{df}(n) = & 1503.58 + 172.77\cos(\hat{\omega}t) - 971.61\cos(2\hat{\omega}t) - 124.13\cos(3\hat{\omega}t) \\ & - 23.55\cos(4\hat{\omega}t) - 42.29\cos(5\hat{\omega}t) - 18.26\cos(6\hat{\omega}t) - 3.61\cos(7\hat{\omega}t) + 29.90\cos(8\hat{\omega}t) \\ & + 5.86\cos(9\hat{\omega}t) + 42.65\cos(10\hat{\omega}t) + 26.45\cos(11\hat{\omega}t) + 10.86\cos(12\hat{\omega}t) \end{aligned} \quad (34)$$

At this point we need the theoretical irradiation functions for the clear-sky models: H_{bh} , which comes from the Hottel model (Equation (18)) and H_{dh} , from the Liu-Jordan model (Equation (21)). These are computed by direct integration of the theoretical irradiance functions.

The daily perturbation coefficients are then:

$$PC_b^n = \frac{H_{bf}(n)}{H_{bh}(n)}; PC_d^n = \frac{H_{df}(n)}{H_{dh}(n)} \quad (35)$$

and with them we finally obtain the perturbed irradiance models:

$$\mathbb{I}_{bh}(n, T) = I_{bh}(n, T) \cdot PC_b^n \quad (36)$$

$$\mathbb{I}_{dh}(n, T) = I_{dh}(n, T) \cdot PC_d^n \quad (37)$$

We start the graphical description of results with the beam

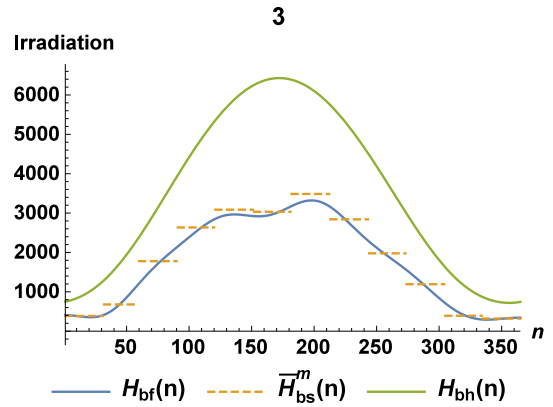


Fig. 1. Satellite estimation \bar{H}_{bs}^m , adjusted H_{bf} , and theoretical H_{bh} irradiation.

radiation. Fig. 1 contains the plots of $\bar{H}_{bs}^m(n)$, $H_{bf}(n)$ (the Fourier polynomial of degree 12 used to approximate $\bar{H}_{bs}^m(n)$), and $H_{bh}(n)$ (W/m^2 /day), which is the theoretical daily distribution of beam solar irradiation given by the Hottel model; the plot covers a year $n = 1, \dots, 365$.

Fig. 2 shows the two values of beam irradiance (W/m^2) at solar noon, that is $T = 12$: $I_{bh}(n, 12)$ for the Hottel model and $\mathbb{I}_{bh}(n, 12)$ for the perturbed model.

In Figs. 3 and 4 the same plots are given for the diffuse irradiation.

Notice (right now at a simple visual level) how the discontinuous PVGIS data are very well fit by the Fourier polynomial

and how the theoretical clear-sky models are quite far from the true data. In Section 4, we study the goodness of fit of our model, when comparing its values to the experimental ones from WRDC.

We stress the remarkable difference in Fig. 1 between the beam solar irradiation values provided by PVGIS and the clear-sky model, which are far greater. This is because the clear-sky model does not take cloudiness or any other shading elements into account. Notice also how the clear-sky model has only two inflection points (corresponding to the equinoxes) whereas the true data presents a clear lack of convexity between Spring and Summer (due, most likely, to the cloudiness of Spring).

Fig. 3, on the other hand, shows how the theoretical values of diffuse irradiance are usually much lower than the real ones, precisely because the Hottel model does not take into account cloudiness. Finally, Figs. 2 and 4 show how our model correctly adjusts the lack of convexity and of symmetry of the true data, in contrast to the perfectly shaped theoretical curve.

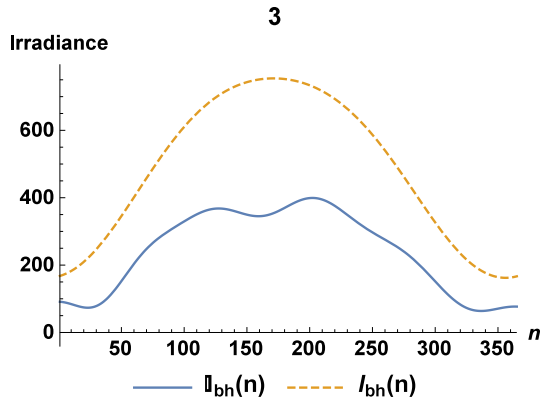


Fig. 2. Adjusted I_{bh} and theoretical I_{bh} irradiance for $T = 12$.

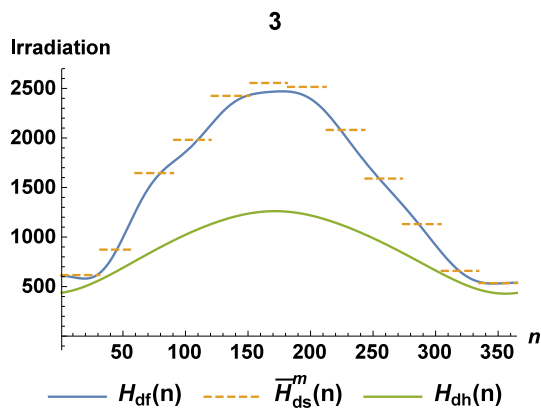


Fig. 3. Satellite estimation \bar{H}_{ds}^m , adjusted H_{df} , and theoretical H_{dh} irradiation.

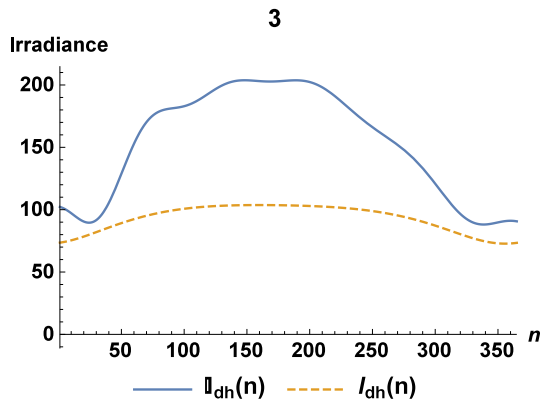


Fig. 4. Adjusted I_{dh} and theoretical I_{dh} irradiance for $T = 12$.

3.2. Summary of results for six cities

We include here the summarized results for the six chosen locations, which belong to latitudes from 36° to 60° North. Thus, we cover all the latitude ranges of the European Climate Zones defined by the NZEB.

In Tables 2 and 3, we provide the Fourier coefficients obtained for each location, which are required to define the corresponding functions $H_{bf}(n)$ and $H_{df}(n)$, respectively. Figs. 5 and 6 gather the corresponding plots: Fig. 5 shows daily values of beam irradiation (left column) and irradiance at noon (right column), while Fig. 6

Table 2
Fourier coefficients a_i of $H_{bf}(n)$ for beam irradiation.

Cities	1	2	3	4	5	6
a_0	4476.86	1986.11	1764.84	1103.18	1206.02	755.391
a_1	279.197	98.0274	204.244	210.253	264.719	164.234
a_2	-2291.36	-1282.74	-1510.84	-980.396	-1316.17	-825.182
a_3	-187.328	-80.1521	-121.157	-207.499	-233.75	-215.53
a_4	-184.786	-87.5333	-55.6244	7.84896	137.428	52.0427
a_5	24.9205	-24.1356	-125.404	7.26317	-38.4792	67.3993
a_6	-15.1567	63.009	62.6737	27.581	26.8608	77.8388
a_7	-49.939	53.1485	83.4012	2.4224	45.8375	-20.321
a_8	8.43416	-47.7465	54.2894	42.0222	-4.78397	-75.4989
a_9	95.9171	-13.7244	-58.6139	39.2357	-58.5892	-12.3567
a_{10}	198.933	47.9965	43.6117	-23.1641	20.1261	62.1661
a_{11}	14.8378	79.0238	50.1859	-22.8897	82.8322	59.3987
a_{12}	24.6464	16.2031	16.5524	3.65283	15.01	10.8709

Table 3
Fourier coefficients a_i of $H_{df}(n)$ for diffuse irradiation.

Cities	1	2	3	4	5	6
a_0	1121.72	1556.64	1503.58	1501.75	1294.18	1274.98
a_1	155.541	105.811	172.773	169.451	181.402	174.097
a_2	-397.745	-860.503	-971.612	-1154.25	-1235.59	-1287.45
a_3	-135.601	-33.4797	-124.129	-100.433	-109.37	-142.541
a_4	-43.9826	35.7292	-23.5482	-11.4527	49.7589	84.0568
a_5	-73.9628	-43.9483	-42.298	-74.1795	-76.3396	-32.6241
a_6	-22.5274	-12.0927	-18.2578	7.84464	-6.0078	4.74353
a_7	44.9484	-4.29593	-3.61199	26.2797	14.7053	-0.246708
a_8	18.8433	-45.8628	29.8982	-2.96431	22.4768	-14.5981
a_9	-37.0028	-15.755	5.86139	-5.42537	3.46068	9.94276
a_{10}	46.3967	95.677	42.6488	51.715	38.1176	60.9544
a_{11}	46.9924	37.7102	26.4452	44.9967	45.0682	43.5623
a_{12}	9.15202	12.9872	10.8591	13.8244	13.428	14.0856

contains the same plots for diffuse irradiation and irradiance at noon. The numbers over each graph correspond to the cities in Table 1.

4. Validation of the method

We carry out, in this section, the error analysis, which confirms the exactness of our method by comparing our perturbed models with the experimental data at ground level provided by the WRDC database [45]. We perform two validations: one for the monthly averages of irradiation \bar{H}_{ba}^m and \bar{H}_{da}^m (beam and diffuse, respectively), obtained from WRDC, and another one for the daily averages $H_{ba}(n)$ and $H_{da}(n)$ (ibid.), which are also available at WRDC. The averages are taken throughout a 10 year period.

As is customary, we shall use the following statistical indicators: mean absolute error (MAE), mean absolute percentage error (MAPE) and root mean square error (RMSE) [51]. We also include the coefficient of determination R^2 (which is dimensionless) [52,53]. The following are their definitions:

$$MAE = \frac{1}{N} \sum_{i=1}^N |p_i - a_i|; \quad MAPE = \frac{1}{N} \sum_{i=1}^N \left| \frac{p_i - a_i}{a_i} \right| \times 100 \quad (38)$$

$$RMSE = \sqrt{\frac{\sum_{i=1}^N (p_i - a_i)^2}{N}}; \quad R^2 = 1 - \left(\frac{\sum_{i=1}^N (p_i - a_i)^2}{\sum_{i=1}^N (a_i - \bar{a})^2} \right) \quad (39)$$

where p_i is the i -th predicted value, a_i the i -th actual measured value, \bar{a} is the mean value of the observed values, and N is the total number of observations.

Notice that the coefficient of determination R^2 cannot be

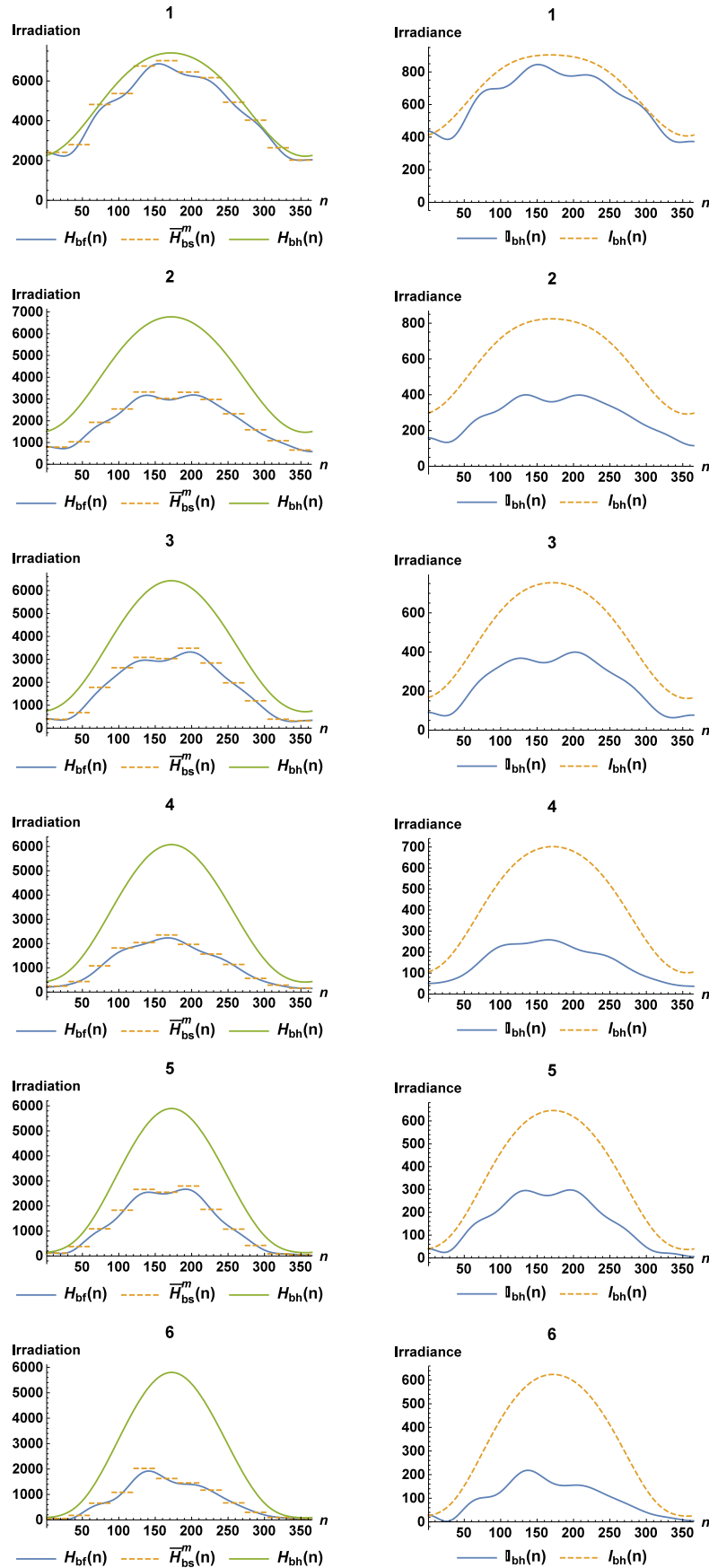


Fig. 5. Collected plots of beam irradiation (left) and beam irradiance at noon (right).

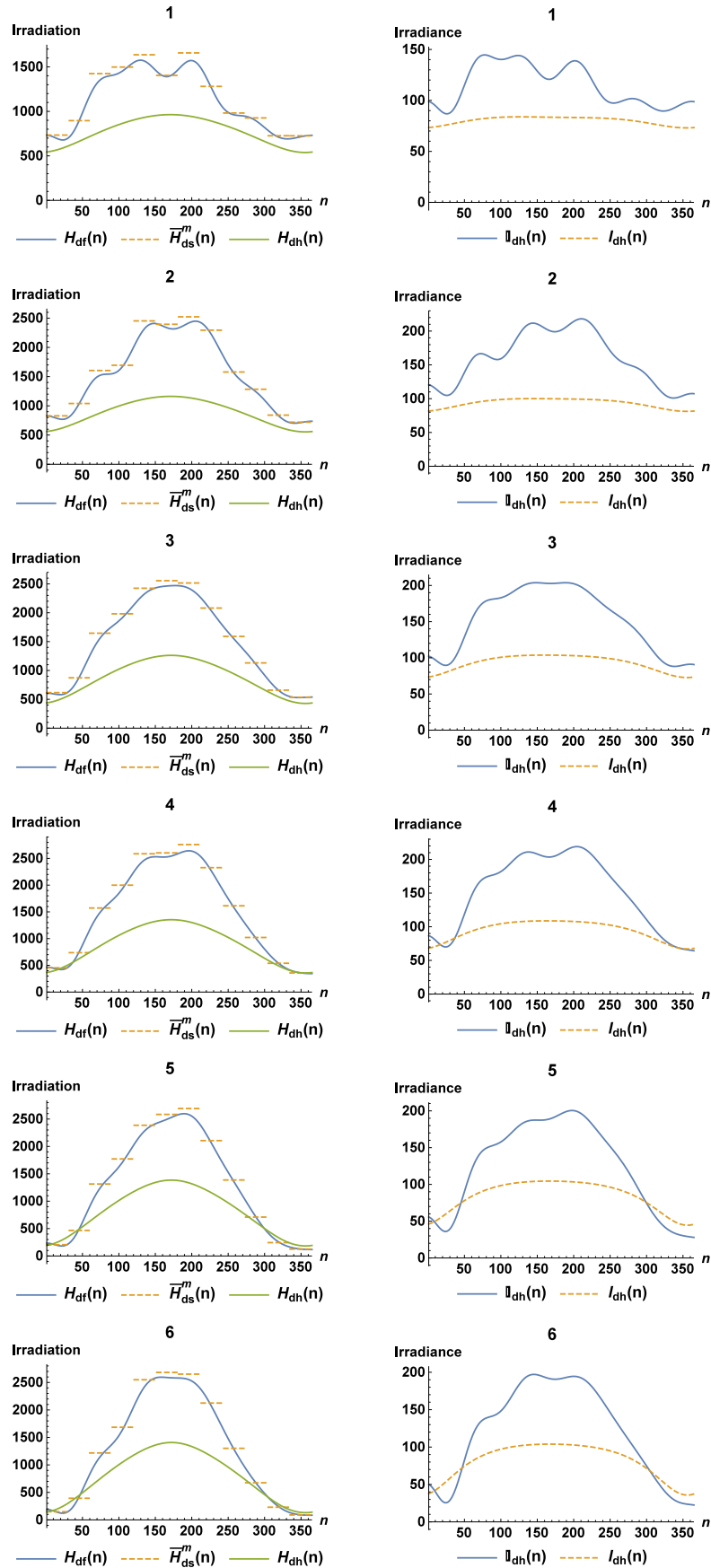


Fig. 6. Collected plots of diffuse irradiation (left) and beam irradiance at noon (right).

Table 4
Error statistics for the perturbed models in monthly beam averages.

	City	MAE	MAPE	RMSE	R ²
1	Desert Rock (USA)	208.584	5.44432	251.710	0.977218
2	Rock Springs (USA)	146.271	12.6625	171.964	0.968648
3	Wien (Austria)	193.437	17.1003	222.432	0.966979
4	Valentia (Ireland)	173.096	13.8662	217.728	0.923166
5	Tartu (Estonia)	228.898	14.1806	334.118	0.922172
6	Lerwick (UK)	72.2964	11.0709	107.908	0.967067

Table 5
Error statistics for the perturbed models in monthly diffuse averages.

	City	MAE	MAPE	RMSE	R ²
1	Desert Rock (USA)	199.251	15.4436	210.590	0.653279
2	Rock Springs (USA)	244.428	13.8842	266.428	0.847770
3	Wien (Austria)	64.4239	4.37843	83.8575	0.986592
4	Valentia (Ireland)	40.3003	3.87426	58.3650	0.995308
5	Tartu (Estonia)	71.0893	9.25022	86.9926	0.988338
6	Lerwick (UK)	176.897	15.1322	215.188	0.956095

Table 6
Error statistics for the perturbed models in daily beam averages.

	City	MAE	MAPE	RMSE	R ²
1	Desert Rock (USA)	459.710	12.7264	582.488	0.889669
2	Rock Springs (USA)	439.447	41.0002	579.395	0.731938
3	Wien (Austria)	363.137	42.7336	497.062	0.857130
4	Valentia (Ireland)	314.783	28.9014	475.871	0.737128
5	Tartu (Estonia)	339.289	148.512	528.801	0.834450
6	Lerwick (UK)	275.239	57.4731	431.710	0.730671

Table 7
Error statistics for the perturbed models in daily diffuse averages.

	City	MAE	MAPE	RMSE	R ²
1	Desert Rock (USA)	231.112	16.8214	297.165	0.574768
2	Rock Springs (USA)	251.845	14.3123	319.574	0.801710
3	Wien (Austria)	129.702	9.43647	170.926	0.948112
4	Valentia (Ireland)	118.703	9.53936	160.003	0.965111
5	Tartu (Estonia)	124.844	13.1569	175.299	0.954999
6	Lerwick (UK)	161.505	16.6093	232.752	0.937646

interpreted in the same way as for linear models (i.e. as the percentage of explained variation) because of the non-linearity. Nevertheless, it is also used by numerous authors as a measure of the goodness of fit.

4.1. Monthly averages

In our case, the values a_i are those of \bar{H}_{ba}^m and \bar{H}_{da}^m monthly average daily beam and diffuse solar irradiation on a horizontal plane. Table 4 contains the values for the relevant statistics of our perturbed Model for beam irradiation. Table 5 gives the same values for diffuse irradiation.

Notice the following:

1. All the MAPE values are less than 20% and actually most are less than or equal to 15%, which for a weather-related approximation seems quite good.
2. The R² values of the perturbed model are essentially 0.9 or more, which indicates a very good model fit. Desert Rock is the only exception in the diffuse irradiation. When discussing the daily averages, we try to provide an explanation for this fact.

4.2. Daily averages

For many reasons, a reliable predictive method for daily irradiation would be of great value. We are going to show in this section that our method provides a rather reasonably accurate tool despite depending only on 12 data points. In Tables 6 and 7 (beam and diffuse, respectively) we include the values of the same error statistics as in the previous section for the daily averages.

Figs. 7 and 8 contain the plots of true daily averages of irradiation $H_{ba}(n)$ and $H_{da}(n)$ (beam and diffuse, respectively), obtained from WRDC; and the values of our perturbed models $H_{bf}(n)$ and $H_{df}(n)$.

We remark the following:

1. The MAPE values are less than 50%, except in the two northernmost locations, Lerwick, for which it is 57% and Tartu, with 149%. Let us explain these values in detail:
 - As long as the daily values are not too small, as happens in the first 4 locations, the MAPE is reasonably good (less than 50%).
 - The high values for Tartu and Lerwick are due to the existence of days with consistent very low (almost 0) beam irradiation (totally overcast days). For instance, day 327 for Tartu has mean daily beam irradiation of 0.27. Just removing this day from the computations changes the MAPE to 65%.
2. The R² values of the perturbed models are all above 0.8 except for (again) the diffuse irradiation in Desert Rock.

For a time series with such high variability as one derived from weather conditions, and a model using just 12 data points, we deem this a very good fit.

The low R² for Desert Rock for diffuse irradiation both in monthly and daily averages might be due to the stark difference in the ratio between direct and diffuse irradiation at that location with respect to the others. Notice, in Figs. 5 and 6 how Desert Rock (1) has values of beam irradiation which are consistently higher (and much higher in the Summer) than those of diffuse irradiation, in clear contrast with all the other locations.

Tables 6 and 7 show that our model for beam irradiation is consistently good at all locations, whereas for the diffuse one, it is less precise at the locations with the lowest latitude (Desert Rock and Rock Springs). However, we cannot establish a specific conjecture for this behavior yet, as there are many other parameters (elevation, orography, proximity to the sea ...) which affect the outcome.

5. Conclusions

One of the key elements in the installation of solar technologies is an accurate predictor of beam and diffuse solar irradiance at the specific location. In market terms, this means having a good estimate of monthly solar irradiation, as this is the elementary budgeting item once the system is deployed.

In this work, a new method for obtaining very accurate models to predict the beam and diffuse horizontal irradiances is proposed.

We develop a novel technique which uses the Fourier expansion [39] applied to the monthly mean irradiation as estimated by the PVGIS system. The obtained Fourier polynomial divided by the theoretical daily irradiation provided by the Hottel model gives a daily perturbation coefficient which has the quality of being "trend-sensitive": as the weather becomes more or less sunny throughout the year, the coefficient increases or decreases accordingly. Another good property is that this perturbation coefficient is, in fact, a continuous

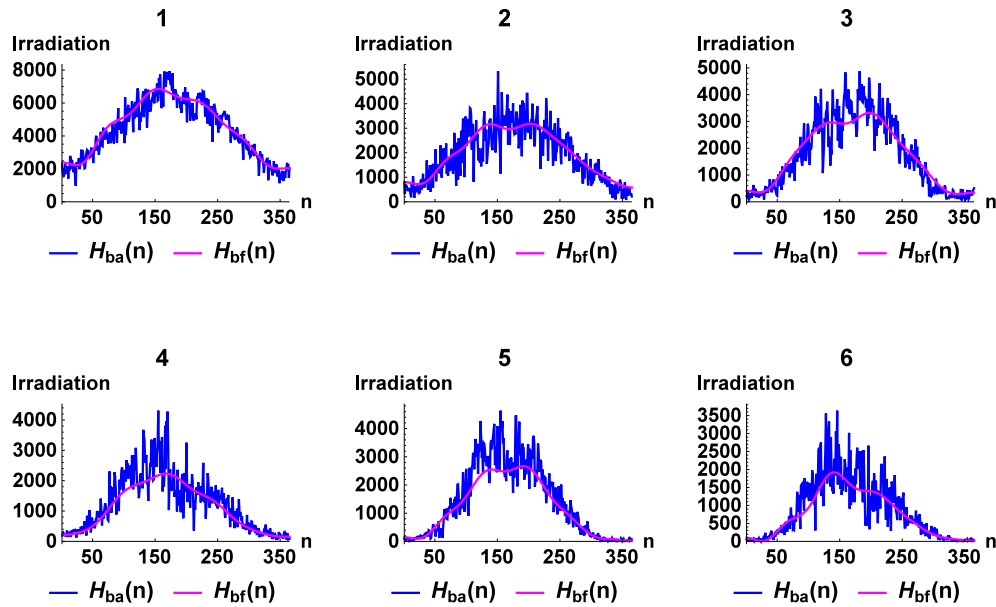


Fig. 7. Daily comparison for beam irradiation.

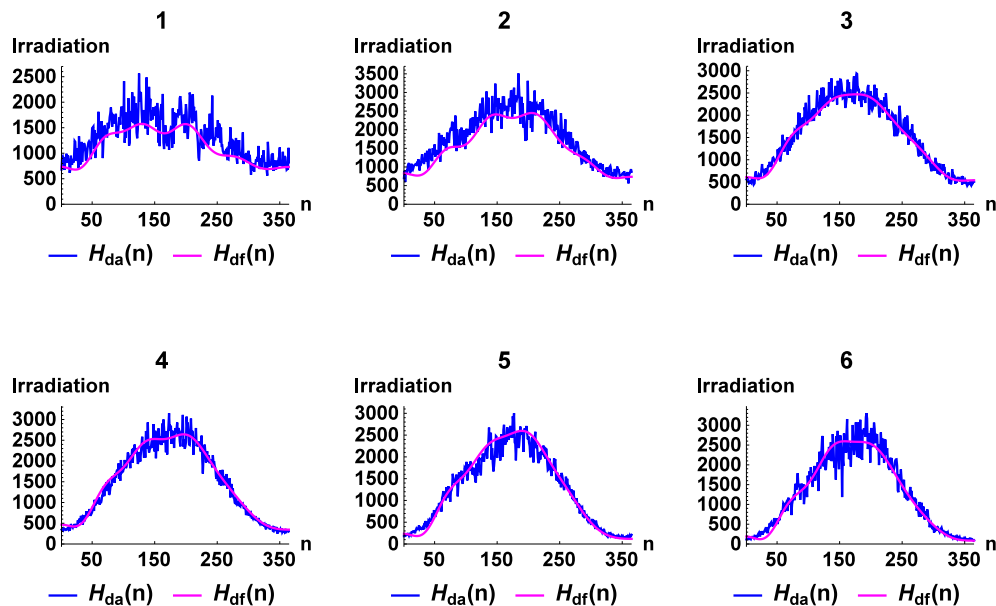


Fig. 8. Daily comparison for diffuse irradiation.

function of the day of the year, which embodies the normally “continuous” nature of weather changes. In order to compute our model, we only need a pair of data for each month: the average solar irradiation (beam and diffuse) per month; we devise an algorithm whose output is 12 numbers (the Fourier coefficients of a cosine series of degree 12) which serve to adjust the Hottel and Liu-Jordan models for irradiance using a daily perturbation coefficient.

We test our model at six locations, using 10 years of actual data obtained from ground-level stations, using the publicly available WRDC database. The error analysis shows a remarkably good fit of our model to the ground-level data, by considering the low values of the *MAPE* and the high values of *R*² both for the beam and the diffuse irradiation models.

Our perturbed model provides, then a rather good, stable and universal predictor for expected monthly and daily irradiation

values, adjusted to each location and type of climate.

We deem our technique easy to implement from readily available data and we remark that it is valid for both any geographical location and any theoretical irradiance model (as the theoretical model is just multiplied by a daily coefficient).

The real irradiation data can be obtained from any database (we have used the one that best fit our study but the technique is exactly the same for any other).

Declaration of competing interest

The authors declare that they have no known competing financial interests or personal relationships that could have appeared to influence the work reported in this paper.

CRedit authorship contribution statement

A. Barbón: Conceptualization, Methodology. **P. Fortuny Ayuso:** Software, Methodology, Writing – original draft. **L. Bayón:** Software, Methodology. **J.A. Fernández-Rubiera:** Data curation, Validation.

Acknowledgments

We wish to thank Dr. Miguel C. Brito for his contribution in this paper.

References

- [1] BP statistical review of world energy, 68th edition, Available at: <https://www.bp.com/content/dam/bp/business-sites/en/global/corporate/pdfs/energy-economics/statistical-review/bp-stats-review-2019-full-report.pdf>, 2019.
- [2] European council report. https://www.consilium.europa.eu/uedocs/cms_data/docs/pressdata/en/ec/145397.pdf. (Accessed 15 October 2019).
- [3] V. Badescu, Modeling Solar Radiation at the Earth's Surface, first ed., Springer, Verlag–Berlin, 2008.
- [4] J. Polo, G. Estalayo, Impact of on-site atmospheric water vapor estimation methods on the accuracy of local solar irradiance predictions, *Sol. Energy* 115 (2015) 621–631.
- [5] J. Zhang, L. Zhao, S. Deng, W. Xu, Ying Zhang, A critical review of the models used to estimate solar radiation, *Renew. Sustain. Energy Rev.* 70 (2017) 314–329.
- [6] J.-L. Chen, L. He, H. Yang, M. Ma, Q. Chen, S.-J. Wu, Z.-L. Xiao, Empirical models for estimating monthly global solar radiation: a most comprehensive review and comparative case study in China, *Renew. Sustain. Energy Rev.* 108 (2019) 91–111.
- [7] L. Mazorra Aguiar, J. Polo, J.M. Vindel, A. Oliver, Analysis of satellite derived solar irradiance in islands with siteadaptation techniques for improving the uncertainty, *Renew. Energy* 135 (2019) 98–107.
- [8] A. Murata, H. Ohtake, T. Oozeki, Modeling of uncertainty of solar irradiance forecasts on numerical weather predictions with the estimation of multiple confidenceintervals, *Renew. Energy* 117 (2018) 193–201.
- [9] A. Khosravi, R.O. Nunes, M.E.H. Assad, L. Machado, Comparison of artificial intelligence methods in estimation of dailyglobal solar radiation, *J. Clean. Prod.* 194 (2018) 342–358.
- [10] A. Teke, H. Başak Yıldırım, Ö. Çelik, Evaluation and performance comparison of different models for the estimation of solar radiation, *Renew. Sustain. Energy Rev.* 50 (2015) 1097–1107.
- [11] F. Antonanzas-Torres, R. Urraca, J. Polo, O. Perpiñán-Lamigueiro, R. Escobara, Clear sky solar irradiance models: a review of seventy models, *Renew. Sustain. Energy Rev.* 107 (2019) 374–387.
- [12] ASHRAE Handbook: HVAC Applications. Chapter 32, ASHRAE, Atlanta (GA), 1999.
- [13] G.S. Campbell, J.M. Norman, An Introduction to Environmental Biophysics, second ed., Springer, New York, 1998.
- [14] H.C. Hottel, A simple model for estimating the transmittance of direct solar radiation through clear atmosphere, *Sol. Energy* 18 (1976) 129–134.
- [15] B.Y.H. Liu, R.C. Jordan, The interrelationship and characteristic distribution of direct, diffuse and total solar radiation, *Sol. Energy* 4 (3) (1960) 1–19.
- [16] E.G. Laue, The measurement of solar spectral irradiance at different terrestrial elevations, *Sol. Energy* 13 (1970) 43–50. IN1-IN4,51-57., [A.B. Meinel, M.P. Meinel, Applied solar energy: an introduction. Addison-Wesley Pub. Co. 1976.
- [17] A.B. Meinel, M.P. Meinel, Applied Solar Energy: an Introduction, Addison-Wesley Pub. Co., 1976.
- [18] C. Perrin de Brichambaut, Estimation des ressources énergétiques solaires en France, Edition Européennes Thermique et Industrie, Paris, 1975.
- [19] J. Nou, R. Chauvin, S. Thil, J. Eynard, S. Griefu, Clear-sky irradiance model for real-time sky imager application, *Energy Procedia* 69 (2015) 1999–2008.
- [20] A. Maafi, S. Harrouni, Preliminary results of the fractal classification of daily solar irradiances, *Solar, Energy* 75 (2003) 53–61.
- [21] V. Bone, J. Pidgeon, M. Kearney, A. Veeraragavan, Intra-hour direct normal irradiance forecasting through adaptive clear-skymodelling and cloud tracking, *Sol. Energy* 159 (2018) 852–867.
- [22] P. Neichen, A broadband simplified version of the solis clear sky model, *Sol. Energy* 82 (2008) 758–762.
- [23] S. Quesada-Ruiz, Y. Chu, J. Tovar-Pescador, H. Pedro, C. Coimbra, Cloudtracking methodology for intra-hour DNI forecasting, *Sol. Energy* 102 (2014) 267–275.
- [24] R. Kostic, J. Mikulovic, The empirical models for estimating solar insolation in Serbia by using meteorological data on cloudiness, *Renew. Energy* 114 (2017) 1281–1293.
- [25] J. Petrzala, L. Komar, M. Kocifaj, An advanced clear-sky model for more accurate irradiance andillumination predictions for arbitrarily oriented inclined surfaces, *Renew. Energy* 106 (2017) 212–221.
- [26] X. Zhong, J. Kleissl, Clear sky irradiances using REST2 and MODIS, *Sol. Energy* 116 (2015) 144–164.
- [27] Y. Dazhi, P. Jirutitjaroen, W.M. Walsh, The Estimation of clear sky global horizontal irradiance at the Equator, *Energy Procedia* 25 (2012) 141–148.
- [28] A. Ianetz, A. Kudish, A method for determining the solar global and defining the diffuse and beam irradiation on a clear day, in: V. Badescu (Ed.), Modeling Solar Radiation at the Earth's Surface, Springer, Verlag–Berlin, 2008.
- [29] C.L. Fu, H.Y. Cheng, Predicting solar irradiance with all-sky image features via regression, *Sol. Energy* 97 (2013) 537–550.
- [30] A. Alzahrani, J.W. Kimball, C. Dagli, Predicting solar irradiance using time series neural networks, *Procedia Computer Science* 36 (2014) 623–628.
- [31] F.V. Gutierrez-Corea, M.A. Manso-Callejo, M.P. Moreno-Regidor, M.T. Manrique-Sancho, Forecasting short-term solar irradiance based on artificial neural networks and data from neighboring meteorological stations, *Sol. Energy* 134 (2016) 119–131.
- [32] Y. Hirata, K. Aihara, Improving time series prediction of solar irradiance after sunrise: comparison among three methods for time series prediction, *Sol. Energy* 149 (2017) 294–301.
- [33] D.H. Li, J.C. Lam, Predicting solar irradiance on inclined surfaces using sky radiance data, *Energy Convers. Manag.* 45 (11–12) (2004) 1771–1783.
- [34] A. Mellit, H. Eleuch, M. Benganem, C. Elaoun, A.M. Pavan, An adaptive model for predicting of global, direct and diffuse hourly solar irradiance, *Energy Convers. Manag.* 51 (4) (2010) 771–782.
- [35] PVGIS. Joint Research Centre (JRC), Available on line at 2019, http://re.jrc.ec.europa.eu/pvg_tools/en/tools.html#PVP.
- [36] NREL. National renewable energy laboratory, Available on line at 2019, https://rredc.nrel.gov/solar/old_data/nsrdb/.
- [37] SOLCAST, Available on line at 2019, <https://solcast.com/>.
- [38] Meteonorm, Available on line at 2019, <https://meteonorm.com/>.
- [39] J. Fourier, A. Freeman, The Analytical Theory of Heat, Dover Publications, New York, 2003.
- [40] A. Ralston, P. Rabinowitz, A First Course in Numerical Analysis, second ed., Dover Publications, New York, 2003.
- [41] J.W. Spencer, Fourier series representation of the position of the sun, *Search* 2 (5) (1971) 172.
- [42] E. Kaplani, S. Kaplanis, S. Mondal, A spatiotemporal universal model for the prediction of the global solar radiation based on Fourier series and the site altitude, *Renew. Energy* 126 (2018) 933–942.
- [43] BSRN. Baseline surface radiation network, Available on line at 2019, <https://bsrn.awi.de/>.
- [44] GEBA. Global energy balance archive, Available on line at 2019, <https://geba.ethz.ch/>.
- [45] WRDC. World radiation data Centre, Available on line at 2019, <http://wrdc.mgo.rssi.ru/>.
- [46] R. Walraven, Calculating the position of the sun, *Sol. Energy* 20 (1978) 393–397.
- [47] J.A. Duffie, W.A. Beckman, Solar Engineering of Thermal Processes, fourth ed., John Wiley & Sons, New York, 2013.
- [48] T.P. Chang, The Sun's apparent position and the optimal tilt angle of a solar collector in the northern hemisphere, *Sol. Energy* 83 (2009) 1274–1284.
- [49] C. Stanciu, D. Stanciu, Optimum tilt angle for flat plate collectors all over the World - a declination dependence formula and comparisons of three solar radiation models, *Energy Convers. Manag.* 81 (2014) 133–143.
- [50] N.D. Kaushika, R.K. Tomar, S.C. Kaushik, Artificial neural network model based on interrelationship of direct, diffuse and global solar radiations, *Sol. Energy* 103 (2014) 327–342.
- [51] R.J. Stone, Improved statistical procedure for the evaluation of solar radiation estimation models, *Sol. Energy* 51 (1993) 289–291.
- [52] Y. El Mghouchi, T. Ajzoul, A. El Bouardi, Prediction of daily solar radiation intensity by day of the year in twenty-four cities of Morocco, *Renew. Sustain. Energy Rev.* 53 (2016) 823–831.
- [53] Y. El Mghouchi, T. Ajzoul, D. Taoukil, A. ElBouardi, The most suitable prediction model of the solar intensity, on horizontal plane, at various weather conditions in a specified location in Morocco, *Renew. Sustain. Energy Rev.* 54 (2016) 84–98.